



Thermomechanical modeling of the metallic rivet in friction riveting of amorphous thermoplastics

Gonçalo Pina Cipriano^{1,2} · Willian S. de Carvalho¹ · Pedro Vilaça² · Sergio T. Amancio-Filho¹

Received: 18 June 2020 / Accepted: 7 December 2020 / Published online: 21 January 2021
© The Author(s) 2021

Abstract

The present work aims for an initial computational simulation with finite element analysis of the friction riveting process. Knowledge and experimental data from friction riveting of AA2024-T351 and polyetherimide supported the computational simulation. Friction riveting is a friction-based joining technology capable of connecting multiple dissimilar overlapping materials in a fast and simple manner. In this paper, the plastic deformation of the metallic rivet, process heat input, and temperature distribution were modeled and simulated. The plastic deformation of the metallic rivet is of key importance in creating the mechanical interlocking and main joining mechanism between the parts, being this the focus of this work. The influence of the polymeric material was considered a dynamic boundary condition via heat input and pressure profiles applied to the rivet. The heat input, mainly generated by viscous dissipation within the molten polymer, was analytically estimated. Three experimental conditions were simulated. The heat flux values applied in modeling of the different conditions were determined (8.2, 9.1, and 10.2 W/mm²). These yielded distinct plastic deformations characterized by a diameter of the rivet tip, from the initial 5 mm to 6.2, 7.0, and 9.3 mm. The maximum temperatures were 365, 395, and 438 °C, respectively.

Keywords Friction · Riveting · Finite element modeling · Temperature · Hybrid

1 Introduction

The field of dissimilar and hybrid connections has nowadays a great importance for several industries, and it is continuously challenging the more traditional methods, e.g., mechanical fastening and adhesive bonding, for their applications. Given this growing interest for alternative joining technologies, it is ever more crucial to have not only deep knowledge regarding the processes on an experimental/practical level but also being able to simulate the mechanisms present during those. This can lead to more lean and efficient methodologies for the

application of such hybrid connections, pushing the envelope on the usage of less conventional materials, having fewer constraints posed by the limitations of these new alternative joining technologies.

Friction riveting is one of such new alternative technologies. Developed and patented by Helmholtz-Zentrum Geesthacht [1], this joining process consists of a rotating cylindrical metallic rivet being pressed against overlapping polymeric components, generating heat by friction and creating metallic insert spot joints. Polymers with and without fiber reinforcements and both thermoplastics and thermosets have been successfully joined [2–5].

The extreme effects that small parameter variation can have on the final deformed geometry of the rivet tip (joint formation) have been investigated and reported by Pina Cipriano et al. [3, 6, 7]. The friction riveting is a fully transient process, encompassing dissimilar materials with quite different physical behavior and temperature dependent properties. During the friction riveting, the temperature evolves from room temperature to peak values in the range from $1.4T_g$ to $0.9T_m$ [2–4, 8]. The heat generation depends on high shear rates, initially localized mostly in the polymer-based component, but arising to the metallic component in the later stages of the process.

Recommended for publication by Commission III-Resistance Welding, Solid State Welding, and Allied Joining Process

✉ Pedro Vilaça
pedro.vilaca@aalto.fi

¹ Institute of Materials Science, Joining and Forming, BMK Endowed Professorship for Aviation, Graz University of Technology, 8010 Graz, Austria

² Department of Mechanical Engineering, School of Engineering, Aalto University, 02150 Espoo, Finland

Therefore, the numerical simulation of the friction riveting process is quite complex and computationally demanding, as it couples geometric, material, and formulation's non-linearity. Thus, simplifications and assumptions must be made. Considering the number of works and investigations into new possible applications and material combinations using friction riveting process [5, 9], it is of great importance that the understanding of the process also be developed from a computational modeling stand point.

This work presents the first study using as research tool the numerical simulation of the friction riveting process applied to AA2024-T351 and polyetherimide (PEI), given the mechanical properties and application of these materials in aircraft industry. The numerical modeling analyses were developed using the Abaqus software. The temperature evolution of the polymeric material, being expelled during the production and geometric characterization of joint consolidation, was registered and evaluated for a given set of process parameters. The former was used as a base for an input in the finite element model (FEM) and the latter as a comparison and validation tool.

2 Materials and methods

2.1 Materials

The metallic rivets used to perform the joints were produced from extruded rods of AA2024-T351. The featureless (plain smooth) cylindrical rivets were 5 mm of diameter and 60 mm of length. Some relevant mechanical properties are shown in Table 1.

The polymeric material used as a base plate for the metallic insert spot joints produced was PEI. The plates were cut into $70 \times 70 \text{ mm}^2$ specimens with 13.4 mm of nominal thickness, from extruded plates (Quadrant Engineering Plastic Products, Germany). It is important to mention that this is an engineering plastic with a glass transition temperature (T_g) of about $215 \text{ }^\circ\text{C}$ [11]. These materials have been addressed with greater depth in the previously published literature regarding the experimental part related to this work [3, 6, 7].

2.2 Friction riveting joining process

The friction riveting process, in the configuration used for the joints investigated in this work, involves a cylindrical metallic

rivet being pressed in a normal direction against the surface of the amorphous thermoplastic part, while rotating at constant rotational speed (RS). Given the low thermal conductivity of the polymer, the heat initially generated by solid friction melts or softens the polymer and allows the insertion of the metal. At this stage, heat is mostly generated by internal shearing and viscous dissipation within the polymer component. This greatly increases the local temperature of the metal, at the penetrating tip of the rivet during the friction time (FT), allowing the plasticizing of the material and its subsequent deformation inside the polymer. The final deformation can be further increased by increasing the axial load applied to the rivet, from a previously constant friction force (FF) to a forging force (FoF), during a forging time (FoT). This last phase of the process was used for the joints currently investigated, but it is not strictly necessary to perform a successful connection as has been demonstrated by Pina Cipriano et al. [7], where the authors studied how a reduction of applied load process requirements can be advantageous, despite resulting in lower mechanical performance when compared to the use of a forging phase.

Figure 1 represents the phases of the process. It is schematically represented how the rivet deforms during the process and which are the assumed conditions of both pressure and heat flux that lead to such material behavior (detailed in Fig. 1 b and c).

On the detail of Fig. 1b, it is schematically represented how the distributions of both heat flux ($q_{(r)}$) and pressure ($p_{(r)}$) are assumed for the short initial stage of the process, as the rivet begins to be inserted into the polymeric material. At this point, the heat flux is assumed to be higher at the outer radius, given the friction between solid surfaces that occurs prior to the melting or softening of the unreinforced polymer. The detail of Fig. 1c illustrates how the heat flux is assumed to have the same type of distribution along the radius as the pressure, since process transitions to a steady-state phase. This will be further discussed in Section 2.6.

2.3 Joint formation and investigated joining conditions

The joint formation of the specimens investigated has been reported in literature [3]. The connections were produced using a friction riveting joining equipment: RNA, H. Loitz-Robotik, Hamburg, Germany. The equipment was custom build for lab-scale purposes, having a maximum rotational speed of 21,000 rpm and 24 kN of axial force. The non-destructive analysis performed by X-ray micro-tomography (Seifert Isovolt 320/13, Russia) allowed a geometrical characterization of the plastic deformation that underwent by the rivet tip as a result of the friction riveting process. The measurement used in this work as a comparison criterion is the maximum width of the deformed rivet tip (W).

Table 1 Selected AA2024-T351 properties [10]

$R_{0.2}$ [MPa]	R_m [MPa]	E [GPa]	Poisson's ratio	Melting Point [$^\circ\text{C}$]
310	427	72	0.33	518–548

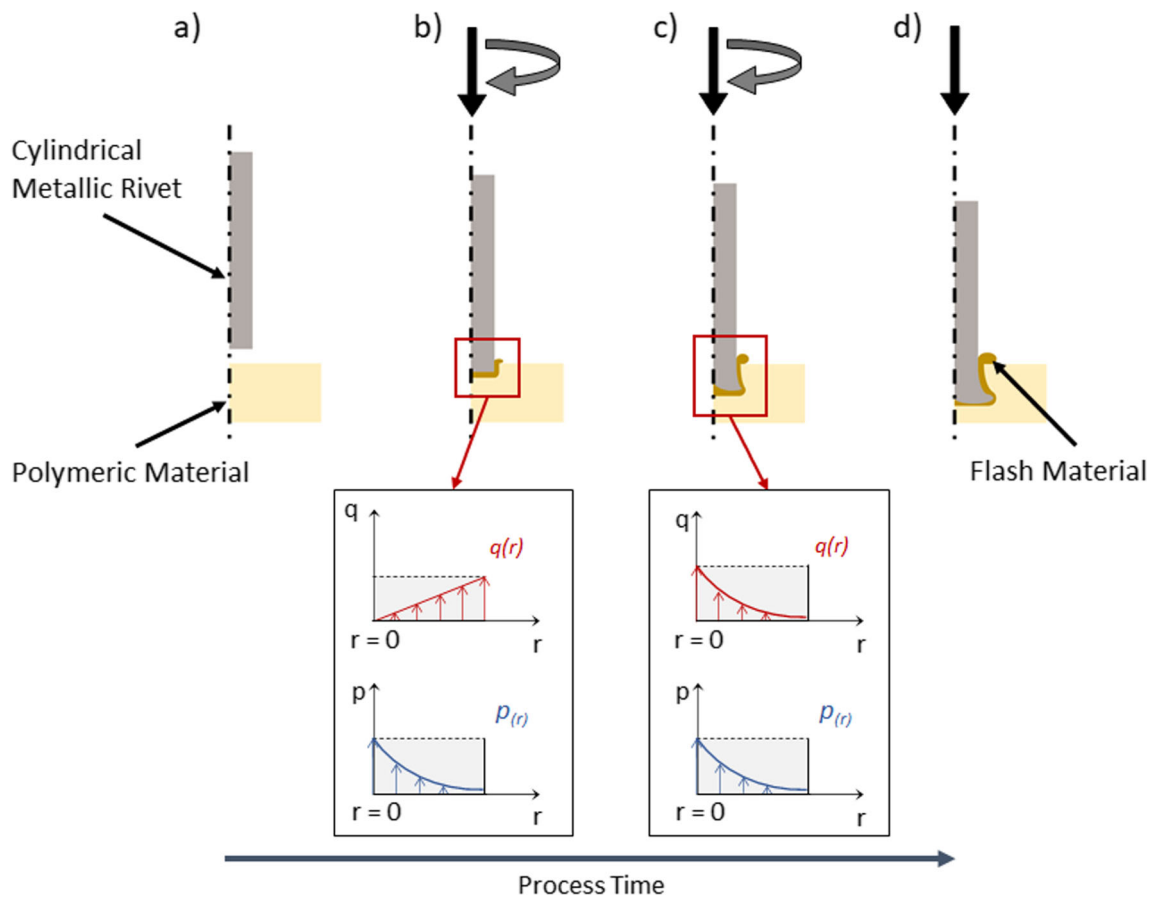


Fig. 1 Schematic representation of the friction riveting process phases in its basic configuration: **a** pre-joining setup; **b** softened/molten polymer layer is formed by the rotation and pressure applied; **c** initial plastic

deformation of tip of the rivet; and **d** final joint consolidation. Detail of exemplifying the profiles of heat flux ($q(r)$) and pressure ($p(r)$) applied by the polymeric material on the rivet tip

The experimental joint specimens, hereby defined as Conditions 1, 2, and 3, investigated in this work were produced using the parameter sets presented in Table 2. These joining conditions were selected from the overall DoE (CCD) performed by Pina Cipriano et al. [3] and represent three highly distinct levels of rivet plastic deformation, presented in Section 3.3 of the present work.

2.4 Process temperature and statistical analysis

The process temperature was assessed by measuring the temperature of the expelled polymeric flash material, resulting from the insertion and deformation of the rivet [3]. The maximum achieved temperatures were determined from the data

collected via infrared thermometry during the process: high-end camera series ImageIR, Infratech GmbH, Germany. The statistical significance of all terms was evaluated at each iteration step by a stepwise backward elimination procedure, within a response surface methodology, which was used to establish a predictive model for the process temperature as a function of the process parameters used in this combination of materials and parameter windows. The same methodology that has been used and previously published for other process responses was applied in the present work for the process temperature [3]. Figure 2 shows an example of the thermography measurements carried out during the process, from which the process temperature was determined.

2.5 Energy input

A preliminary heat input model has been reported in literature by Amancio and Dos Santos [8]. This model arising from principles applied to friction welding processes of both metallic and polymeric materials aims to give an estimation of the power being converted into thermal energy during the friction riveting process. The total heat input is considered to arise

Table 2 Parameter sets to produce the investigated joints

Condition	RS [rpm]	FT [s]	FF [N]	FoT [s]	FoF [N]
1	18,000	1.6	2000	1	5100
2	19,000	1.4	2500	1.5	4500
3	20,000	2	2000	1	5100

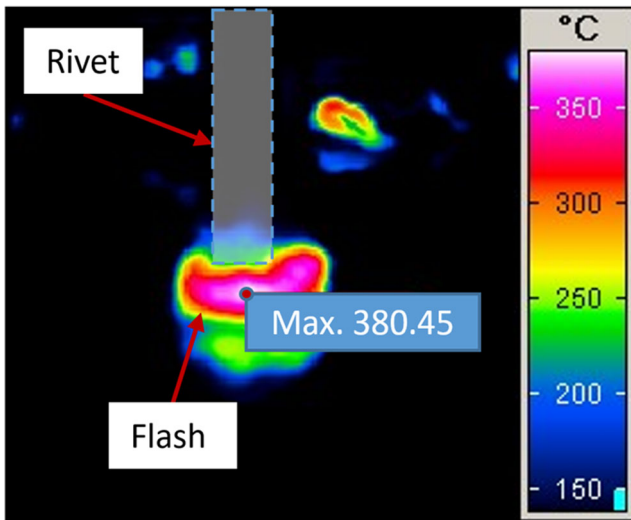


Fig. 2 Infrared thermography used to obtain the maximum process temperature, measured on the material being expelled as flash

from four distinct contributions during the process. Two of these contributions result from the solid friction phase that takes place during the initial instants of the process. The other two contributions arise from viscous state effects, namely, viscous dissipation. Amancio and Dos Santos concluded that the axial contributions, resulting from the normal force applied, were negligible in comparison with the contributions arising from friction, both solid and viscous. The solid contribution, Q_{fr}^{sol} , is determined based on calculations for friction welding of metals and of spin welding of polymers [12]. The proposed final simplification takes the form of

$$Q_{fr}^{sol} [W/m^2] = \frac{2}{3} \cdot \pi \cdot \mu \cdot P(r) \cdot v_{max} \tag{1}$$

where μ represents the kinematic friction coefficient, $P(r)$, the normal pressure distribution over the flat circular area at the rivet tip—in contact with the polymeric plate—and v_{max} is the tangential velocity at the outer radius of the rivet.

The viscous component of the frictional contribution, Q_{fr}^{visc} , arises from the adaptation of the proposed calculation for internal viscous energy dissipation proposed by Potente and Reinke [12]. Given the rheological similarities with the steady-state viscous dissipation phase of the friction riveting process and assuming simple shear deformation, the following equation can be used:

$$Q_{fr}^{visc} [W] = \eta \gamma^2 \cdot Vol \tag{2}$$

where η is the molten state polymer viscosity and γ and Vol are the shear rate and volume of the referred molten polymer, respectively. This equation was rearranged to obtain the value per area.

$$Q_{fr}^{visc} [W/m^2] = \eta \frac{v_{max}^2}{h} \tag{3}$$

Here, h represents the axial depth of molten polymer layer ahead of the rivet tip. The molten polymer viscosity is determined by taking into account both the temperature and shear rate applied to the polymer. Beginning with the determination of the viscosity at a given temperature and absent shear rate, η_T , Amancio and Dos Santos used the Williams-Landel-Ferry equation [13]:

$$\eta_T = \eta_0 \cdot \exp \left[\frac{-C_1 \cdot (T - T_g)}{C_2 + T - T_g} \right] \tag{4}$$

In this equation, η_0 represents the viscosity of the polymer at its transition temperature, T_g ; C_1 and C_2 are material-related constants; and T is the temperature of interest.

Following the proposed modified Cross formulation, by Stokes and Poslinski [14] for polymer spin welding, the viscosity of the molten polymer under shear, η , can be determined with the following equation:

$$\eta = \eta_T \cdot \left[1 + \left(\frac{\eta_T^{-\gamma}}{\tau^*} \right)^\alpha \right]^{\frac{n-1}{\alpha}} \tag{5}$$

Here, τ^* represents the constant related to the point at which the material is in transition to non-Newtonian shear-thinning behavior, α is the breath index of the curve, and n is the power law coefficient associated with rheological behavior of the polymer. Given the low contribution of the axial terms of the model, a simplified equation used by Amancio and Dos Santos is presented in the following form [8]:

$$Q_{total} [W/m^2] = \left[\left(\frac{2}{3} \cdot \pi \cdot \mu \cdot P(r) \right) + \left(\eta \cdot \frac{v_{max}}{h} \right) \right] \cdot v_{max} \tag{6}$$

2.6 Numerical simulation

Using Abaqus software, in the first phase of the work, the deformation experienced by the metallic rivet during the friction riveting process was simulated via a fully coupled thermo-structural analysis, using an axisymmetric model, solved with explicit method. The explicit solving approach was selected due to the high non-linearity character of this model [15]. In this work, the experimental interaction between the metal and the polymer was modeled using a simplified approach. The real total resistance, offered by the polymer, to the advance of the rivet was known, as the process was experimentally investigated using a force-controlled time-limited variant. This load was applied

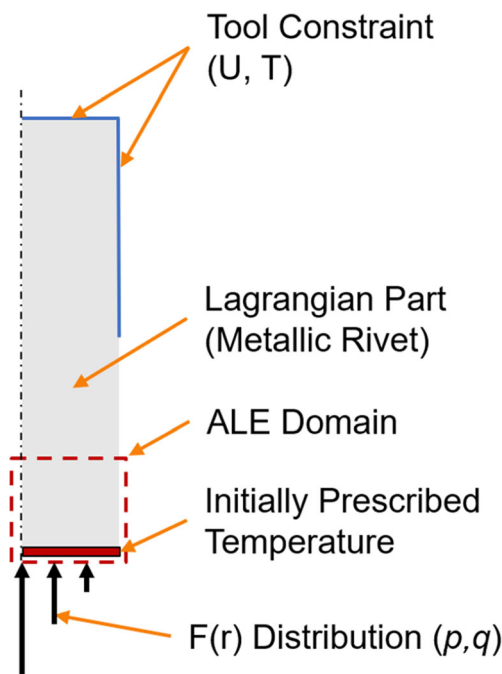


Fig. 3 Schematic representation of the experimental conditions modeled, depicting the applied displacement (U) and temperature (T) constraints and use of radial functions (F(r)) of pressure (p) and heat flux (q)

directly on the top circular surface of the plunged rivet tip, as seen in Fig. 3. Part of the rivet on the opposite side (non-plunged extremity) was constrained, to simulate the experimental setup, where the rivet is clamped by the chuck tool connected to the spindle of the joining equipment.

The heat power was modeled by applying a heat flux resultant from the calculations using the viscous term of Eq. 6. The obtained results were 8.2, 9.1, and 10.2 W/mm², for Conditions 1, 2, and 3, respectively. The initial instantaneous solid friction part of the process was simulated by imposing a temperature equal to the glass transition temperature, $T_g = 215\text{ }^\circ\text{C}$, of the process at the rivet tip surface as an initial condition. The contribution of the rotation of the rivet is the main mechanism generating heat during the experimental process and is taken into account in the shear rate experienced by the molten polymer, and inherent heat generation. Considering the molten polymer flow advancing ahead of the rivet tip, without rotation, it can initially be simplified as a parallel flow against the circular plate of a cylinder, with a stagnation point at the central axis of the rivet. Given this flow velocity radial gradient, the resulting pressure applied to the rivet by the polymer must also be modeled as radius-dependent. For these initial studies, a radial second-order distribution was modeled by a field function ($f(r) = 0.04r^2 - 0.25r + 0.45$) that was used to apply the pressure load.

The metallic material behavior was governed by a Johnson-Cook model (Eq. 7), with the material coefficients used shown in Table 3 [17].

Table 3 Johnson-Cook material model parameters for AA2024-T351 [16]

A [MPa]	B [MPa]	n	C	m	T _m [°C]
369	684	0.73	0.0083	1.7	522

$$\bar{\sigma} \text{ [MPa]} = \left(A + B\bar{\epsilon}^n \right) \left[1 + C \ln \left(\frac{\bar{\epsilon}}{\bar{\epsilon}_0} \right) \right] \left[1 - \left(\frac{T - T_{room}}{T_m - T_{room}} \right)^m \right] \tag{7}$$

The FEM analysis was defined as having two domains, where the plunged tip of the rivet was modeled with adaptive meshing, using arbitrary Lagrangian-Eulerian (ALE) approach. This finite element scheme was selected in order to allow the initial mesh to accommodate the extreme deformation experienced by the rivet. The properties of the material were defined as functions of temperature. A constant room temperature (25 °C) was imposed to the surface of the non-plunged extremity, upper half, of the rivet simulating the clamping by the refrigerated chuck connected to the spindle of the joining equipment.

The mesh established could accommodate the material plastic flow, by making use of an ALE approach to adaptive meshing, at a frequency of one every increment, using an enhanced control algorithm for the evolving geometry at the tip of rivet. Preventing the mesh used from being excessively distorted given the material flow, a reduced integration thermal-stress coupled axisymmetric element was used (CAX4RT). The total number of variables in the model was 12,456. Mass scaling was also applied to the whole model, in order to keep the time increment to 1E-8. These were simplifications necessary to reduce the computational cost of the analysis. The first step of the analysis simulated the friction phase of the process, corresponding to the application of rotation and friction force during a given friction time period. During this step, both pressure and the determined heat flux were applied to the rivet. Following this, a second step was applied, in order to simulate the second experimental phase, designated as a forging phase, during which it is assumed that no heat generation occurs, since experimentally the rotation is brought to a halt, and the metallic rivet further deforms plastically, given the plasticized

Table 4 Parameters for heat input calculations

Input parameter	PEI	Input parameter	PEI
η_0 [Pa.s] [14]	1.83E+13	τ^* [MPa] [14]	1.02
C_1 [14]	31.96	α [14]	0.68
T_g [°C] [11]	215	n [18]	0.32
C_2 [14]	51.6	h [mm]	1

Table 5 Process parameters for heat flux calculations

Condition	γ [s ⁻¹] (T=375 °C)	v_{max} [m/s] (T=375 °C)
1	73.6	3.34
2	77.7	3.52
3	81.8	3.71

state resulting from the friction phase. The heat flux was applied to the rivet tip along the radius using the same distribution as for the pressure ($f(r)$), previously mentioned. The magnitude of energy being transferred to the rivet was determined at an assumed constant temperature (375 °C) in these preliminary investigations on the process simulation.

3 Results and discussions

3.1 Heat input

For the conditions investigated, the heat input was determined using the parameter values of Table 4, applied to Eqs. (4), (5), and (6).

The remaining necessary parameter specific to each experimental condition, shear rate, necessary to determine the heat flux is shown in Table 5, assuming a thickness of 1 mm of molten polymer flow ahead of the rivet tip, under shear. These were determined following the calculations described in Section 2.5. The heat flux was determined at a temperature of 375 °C.

3.2 Rivet plastic deformation computational model

Although higher energy is generated by viscous dissipation at the outer radius of the rivet, since the velocity gradient is higher, the energy transferred to the rivet is assumed to be lower in this region in comparison to the center of the rivet. This is due to the fact that the polymer in this region is expelled as flash material as the rivet is inserted, being continuously replenished by newly molten/softened polymer. On the contrary, at the center axis of the rivet where the pressure is higher, the polymer is expected to transfer more energy to the metallic rivet; hence, it is expected that the metal is achieving higher temperatures at this region, as previously discussed in Section 2.6. This is in accordance with the typical plastic deformation geometry of the metal, which seems to evidence an earlier softening of the material at the center axis than at the

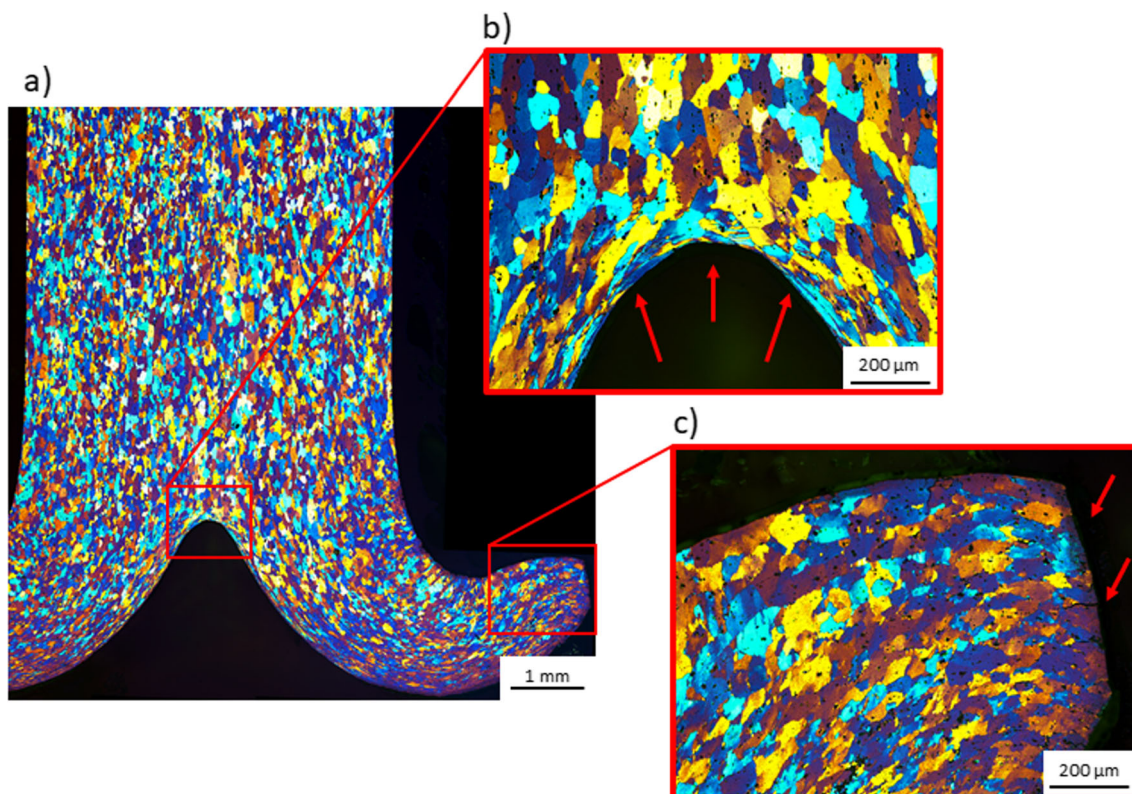


Fig. 4 Example of the metallic rivet microstructure after the plastic deformation during friction riveting (FT, 2.2 s; FF, 3000 N; RS, 19000 rpm; FoT, 1 s; FoF, 4000 N); **a** partial view of the deformed rivet tip; **b** detailed view of the central area of the rivet tip in contact

with the polymer, where dynamic recrystallization microstructural changes can be seen highlighted by arrows; and **c** region of the rivet feature with the highest increase in radius, where no significant changes observed

outer radius. As such, it was assumed that the pressure and temperature accumulation at the inserted tip of the rivet evolve during the process with the changes in the heat flux being generated, from the initial instances, solid friction, to a steady developed process, as represented in Fig. 1. For the purposes of this work, the steady-state developed process mechanisms are considered (Fig. 1c), since these account for most of the energy applied to the rivet [8].

These assumptions were correlated to the material changes experienced by the metal located at the tip of the rivet. Figure 4 represents the typical microstructure of a metallic rivet which undergoes a considerable plastic deformation during friction riveting. The results observed with microstructural analysis corroborate the assumption that the temperature increase in the metallic material is higher at the central region, where highly compacted and also equiaxed, visually smaller grains can be detected in a thin layer at the bottom part of the rivet tip center, evidencing the occurrence of annealing mechanisms, such as partially dynamic recrystallized grains, resulting from the temperatures and strains experienced by the material (Fig. 4b). Although for a different process variant, Amancio [19] has also reported these trends in previous works using the same amorphous thermoplastic and a drawn AA2024-T3 rivet. The fact that at the outermost region (Fig. 4c), the grain structure remains coarse as in the as-received rivet, is evidence that despite the higher speed, given the greater distance to the center, the increase in temperature experienced by the metal appears to be insufficient to promote the occurrence of dynamic recrystallization-dependent grain refinement [20]. Hence, the assumption that both temperature and pressure at the metal are higher at the rivet axis, previously described in Section 2.6 (see also Fig. 1), can be, for the purpose of this study, validated. Additional metallurgical characterization by SEM-EBSD and TEM would be required to confirm these assumptions. Nevertheless, these were out of the scope of this publication.

The plastic deformation at the tip of the rivet was assessed by comparing the increase in diameter observed experimentally and the result of the numerical simulation, the measurement designated as maximum width of the deformed rivet tip (W). The overall geometry of the plastically deformed material was evaluated qualitatively, being the objective to obtain a bell-shaped deformation, characteristic of the materials used when joined by friction riveting without the occurrence of excessive plastic deformation. For the joining conditions being investigated, the predicted process temperature was found to be comparable to the measured values registered experimentally during the joining process by infrared tomography. The predictive model was determined following the same methodology applied in previous works available in literature [3, 6]. The determined equation for the process temperature as a function of the coded values ($[-2, 2]$), with these corresponding to the ranges of the process parameters (FT, [1.4,

2.2] s; FF, [1.5, 3.5] kN; RS, [17,000, 21,000] rpm; FoT, [0.5, 2.5] s; FoF, [3.3, 5.7] kN), of the process parameters is

$$T = 436.04 + 16.21 RS + 20.60 FT + 22.37 FF + 0.61 FoT + 0.55 FoF + 12.21 FoT*FoF \quad (8)$$

The model validation resulted in an adjusted R -squared of 78.2%, with a standard error, S , of 15.3 °C and a predicted R -squared of 74.7%.

Both the experimental and predicted temperature results were found to be in accordance with the maximum temperature values at the center of the rivet tip surface, registered for the simulated process, as a result from the heat flux and pressure profile applied to the rivet tip. This comparison can be seen in Fig. 5, for the three conditions and the three sets of temperatures for each condition.

Small differences between the predicted values and those measured experimentally were observed. A good accuracy

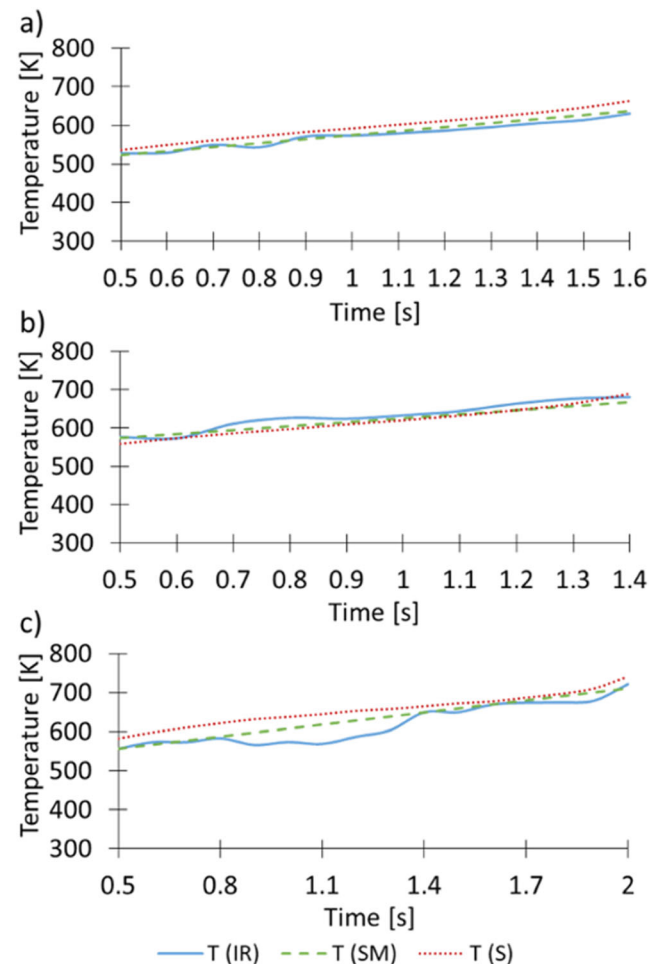


Fig. 5 Plotted comparisons between process temperatures obtained experimentally (IR), predicted by the statistical model (SM), and simulated (S) over the friction phase of the joining time for a Condition 1, b Condition 2, and c Condition 3

between the predicted and simulated results was also observed. One process-associated limitation that can explain the local variations, of the experimental values, is the irregular molten polymer flash material formation and expulsion as the rivet is being inserted [3], varying slightly with increasing rivet insertion and its plastic deformation. These results make it possible to assume that the maximum temperature predictive regression model is an accurate tool to determine the process temperature evolution during joining, as a function of the process parameters, in a simple and analytical manner, for the combination of material being investigated. Also, given the similarity of the temperature values, the assumptions, the approximations, and the determined values for the heat flux applied to the rivet can be considered validated.

The plastic deformation of the rivet tip was characterized by the maximum width of the deformed rivet tip (W). The experimental and simulated results were compared to assess the accuracy of the model. Figure 6 shows the maximum temperature at the end of the friction phase and the final plastically deformed rivet for the simulated process after forging phase.

When compared with the experimental deformation (Fig. 7), it is possible to observe that for Condition 1 (smallest

rivet deformation), the same value for W (6.2 mm), was obtained for both experimental and simulated results. With the increase of energy and deformation, the computational results begin to deviate from the experimental ones. For Condition 2, an experimental W of 7 mm was not well matched by the finite element analysis, which yielded a W of 6.6 mm, although the overall rivet tip's plastic deformation shape was similar. In the case of the condition with the highest deformation (Condition 3), the model was not able to accurately predict the deformation (W). The maximum width measured experimentally was 9.3 mm, while the value resulting from the computational simulation was 8.3 mm. This difference in values may be explained by the fact that some of the assumptions and simplifications considered for the finite element analysis can become not suitable for such plastic deformation. With the increase of plastic deformation experienced by the rivet, the polymeric material being expelled during the process is expected to encounter higher resistance when flowing outwards, as it tends to follow the exterior contour of the metallic deformation (local increase of radius at the rivet tip), rapidly changing the subsequent material response to the process. Not only this but also the fact that a higher volume of material involved

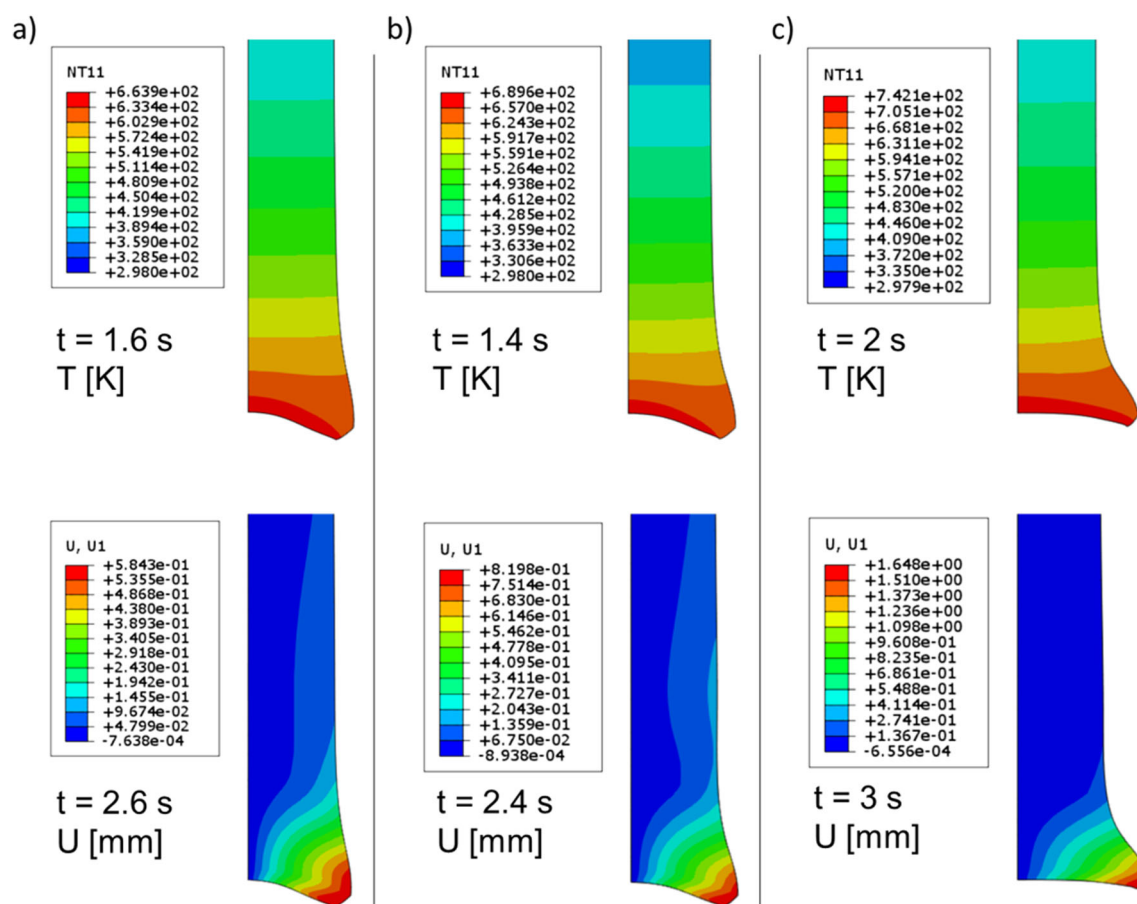


Fig. 6 Simulated process results for both temperature distribution (NT11) and displacement (U) for **a** Condition 1 ($T = 664\text{ }^{\circ}\text{C}$ and $W = 6.2\text{ mm}$), **b** Condition 2 ($T = 690\text{ }^{\circ}\text{C}$ and $W = 6.6\text{ mm}$), and **c** Condition 3 ($T = 742\text{ }^{\circ}\text{C}$ and $W = 8.3\text{ mm}$)

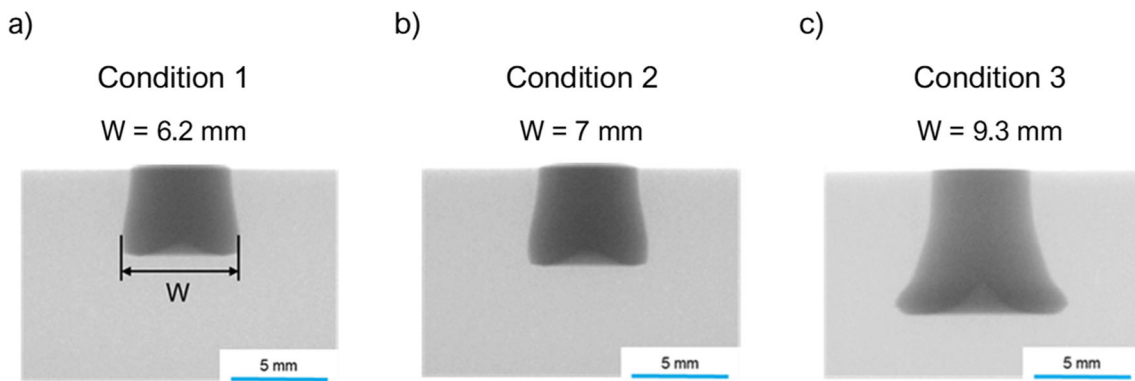


Fig. 7 Comparison between the joint formation obtained experimental and respective computational simulation results for **a** Condition 1, **b** Condition 2, and **c** Condition 3

in heat exchanges is expected to gradually modify the local plastic deformation phenomena. The quantification of these evolutions is expected to become necessary in order to increase the accuracy of future works on a computational model of the process, particularly influencing local changes at outer radius of the rivet.

By increasing the computational resources and refining the boundary conditions applied in this model, it is probable that these results can be improved, achieving a higher accuracy with those obtained experimentally. Despite this fact, it is already possible to state that the model can give a qualitative indication to the mechanical performance of friction riveted connections. This is further reinforced by previous publications which have established good correlations between the plastic deformation of the rivet and the quasi-static mechanical performance of the joint, particularly for the cases investigated here, which constitute energy-efficient connections as defined by Pina Cipriano et al. [6].

4 Conclusions

The present work was able to demonstrate that despite the assumptions and simplifications, it was possible to obtain a good correlation between the simulated plastic deformation of the metallic rivet and the experimental results of the joints produced. As a first investigation on modeling the friction riveting process, the results validated the use of the preliminary heat input model proposed in literature for the process, as a tool for estimating and simulating the energy being delivered to the rivet. This was verified by the good accuracy that the temperature evolution observed computationally demonstrated to the experimental results. Also, the temperature statistical predictive model presented was validated as a good simple analytical tool, capable of yielding the process temperature as a function of the parameters. The assumptions made regarding the heat flux applied to the metallic rivet, specifically that it is highest at the center of the rivet, can be

considered valid, since the resulting simulations demonstrated similar plastic deformation to the experimental results. For higher levels of rivet deformation, further investigations should be carried out in order to improve result accuracy. Given the fact that the plastic deformation occurs considerably fast and at such elevated temperatures, changes on both the adaptive meshing rules and material model used might be necessary in order to improve the accuracy of the computational model for high rivet plastic deformation cases. Once a good correlation between the modeled results and higher plastically deformed conditions is achieved, a qualitative level of mechanical performance can be inferred from the simulation without the need for experimental results, given established correlations published in literature.

Funding Open Access funding provided by Graz University of Technology. The authors would like to acknowledge the financial support provided by the Helmholtz Association, Germany (Grant No. VH-NG-626), the Austrian Aviation Program TAKE OFF, and BMK-Austrian Ministry for Climate Action, Environment, Energy, Mobility, Innovation and Technology.

Open Access This article is licensed under a Creative Commons Attribution 4.0 International License, which permits use, sharing, adaptation, distribution and reproduction in any medium or format, as long as you give appropriate credit to the original author(s) and the source, provide a link to the Creative Commons licence, and indicate if changes were made. The images or other third party material in this article are included in the article's Creative Commons licence, unless indicated otherwise in a credit line to the material. If material is not included in the article's Creative Commons licence and your intended use is not permitted by statutory regulation or exceeds the permitted use, you will need to obtain permission directly from the copyright holder. To view a copy of this licence, visit <http://creativecommons.org/licenses/by/4.0/>.

References

1. Amancio-Filho ST, Beyer M, dos Santos JF (2009) Method of connecting a metallic bolt to a plastic workpiece. US 7575149B2
2. Altmeyer J, dos Santos JF, Amancio-Filho ST (2014) Effect of the friction riveting process parameters on the joint formation and

- performance of Ti alloy/short-fibre reinforced polyether ether ketone joints. *Mater Des* 60:164–176. <https://doi.org/10.1016/j.matdes.2014.03.042>
3. Pina Cipriano G, Blaga L, dos Santos JF et al (2018) Fundamentals of force-controlled friction riveting: part I—joint formation and heat development. *Materials (Basel)*:1–23. <https://doi.org/10.3390/ma11112294>
 4. Borba N, Afonso C, Blaga L, dos Santos J, Canto L, Amancio-Filho S (2017) On the process-related rivet microstructural evolution, material flow and mechanical properties of Ti-6Al-4V/GFRP friction-riveted joints. *Materials (Basel)* 10:184. <https://doi.org/10.3390/ma10020184>
 5. Borba NZ, Kötter B, Fiedler B, dos Santos JF, Amancio-Filho ST (2020) Mechanical integrity of friction-riveted joints for aircraft applications. *Compos Struct* 232:111542. <https://doi.org/10.1016/j.compstruct.2019.111542>
 6. Pina Cipriano G, Blaga L, dos Santos J, Vilaça P, Amancio-Filho S (2018) Fundamentals of force-controlled friction riveting: part II—joint global mechanical performance and energy efficiency. *Materials (Basel)* 11:2489. <https://doi.org/10.3390/ma1122489>
 7. Pina Cipriano G, Ahiya A, dos Santos JF, Vilaça P, Amancio-Filho ST (2020) Single-phase friction riveting: metallic rivet deformation, temperature evolution, and joint mechanical performance. *Weld World* 64:47–58. <https://doi.org/10.1007/s40194-019-00803-3>
 8. Amancio-Filho ST, Dos Santos JF (2016) Preliminary analytical modeling of heat input in friction riveting. In: *Annual Technical Conference - ANTEC, Conference Proceedings*. pp. 1310–1317
 9. Borba NZ, Blaga L, dos Santos JF, Amancio-Filho ST (2018) Direct-friction riveting of polymer composite laminates for aircraft applications. *Mater Lett* 215:31–34. <https://doi.org/10.1016/J.MATLET.2017.12.033>
 10. J.R. Davis & Associates., ASM International. *Handbook Committee (1993) Aluminum and aluminum alloys*. ASM International
 11. Professional Plastics (2011) Duratron U1000 PEI. Quadrant plastics. <https://www.quadrantplastics.com/de/produkte/technische-kunststoffe/temperatur-160-220-c/duratronr-pei/?t=1>. Accessed 2 Oct 2018
 12. Potente H, Reinke M (1981) Welding parameters and properties of polyolefin parts. *Plast Rubber Process Appl* 1:149–160
 13. Tadmor Z, Gogos CG (2007) *Principles of polymer processing*
 14. Stokes VK, Poslinski AJ (1995) Effects of variable viscosity on the steady melting of thermoplastics during spin welding. *Polym Eng Sci* 35:441–459. <https://doi.org/10.1002/pen.760350510>
 15. Harewood FJ, McHugh PE (2007) Comparison of the implicit and explicit finite element methods using crystal plasticity. *Comput Mater Sci* 39:481–494. <https://doi.org/10.1016/j.commatsci.2006.08.002>
 16. Kay GJ (2003) Failure Modelling of titanium 6Al-4V and aluminum 2024-T3 with the Johnson-Cook material model. DOT Rep
 17. Johnson GR, Cook WH (1983) A constitutive model and data for metals subjected to large strains, high strain rates and high temperatures. *7th Int. Symp. Ballist.* 541–547
 18. Dealy JM, Wang J (2013) Melt rheology and its applications in the plastics industry. *Melt Rheol its Appl Plast Ind.* <https://doi.org/10.1007/978-94-007-6395-1>
 19. Amancio-Filho ST (2011) Henry Granjon prize competition 2009 winner category a : “ joining and fabrication technology ” Friction riveting: development and analysis of a new joining technique for polymer-metal multi-material structures. *Weld World* 55:13–24
 20. Davis JR (1993) *ASM specialty handbook: Al and Al alloys*. ASM International

Publisher's note Springer Nature remains neutral with regard to jurisdictional claims in published maps and institutional affiliations.